

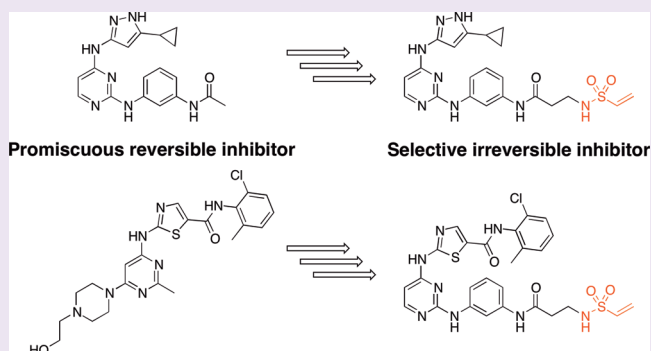
Irreversible Inhibitors of c-Src Kinase That Target a Nonconserved Cysteine

Frank E. Kwarcinski,[†] Christel C. Fox,[†] Michael E. Steffey,[†] and Matthew B. Soellner^{*,†,‡}

[†]Department of Medicinal Chemistry and [‡]Department of Chemistry, University of Michigan, 930 N. University Avenue, Ann Arbor, Michigan, 48109, United States

S Supporting Information

ABSTRACT: We have developed the first irreversible inhibitors of wild-type c-Src kinase. We demonstrate that our irreversible inhibitors display improved potency and selectivity relative to that of their reversible counterparts. Our strategy involves modifying a promiscuous kinase inhibitor with an electrophile to generate covalent inhibitors of c-Src. We applied this methodology to two inhibitor scaffolds that exhibit increased cellular efficacy when rendered irreversible. In addition, we have demonstrated the utility of irreversible inhibitors in studying the conformation of an important loop in kinases that can control inhibitor selectivity and cause drug resistance. Together, we have developed a general and robust framework for generating selective irreversible inhibitors from reversible, promiscuous inhibitor scaffolds.



While reversible small molecule inhibitors of protein kinases have been extensively investigated,^{1–3} irreversible kinase inhibitors remain underexplored.^{4,5} Compared to their reversible counterparts, irreversible kinase inhibitors offer significant advantages, including increased potency and selectivity, longer residence times, the ability to inhibit kinases with existing resistance mutations, and non-ATP-competitive modes of action.^{6,7} Despite these advantages, irreversible kinase inhibitors have only been developed for a handful of kinases.⁶

Herein, we report a series of irreversible c-Src inhibitors. c-Src tyrosine kinase was the first proto-oncogene discovered and is frequently overexpressed in cancerous tumors.^{8,9} The extent of c-Src overexpression typically correlates with the metastatic potential of the malignant tumor, and inhibiting c-Src has been shown to decrease breast cancer metastases in mice.^{8,9} Elevated c-Src activity has recently been identified as a main cause of resistance to Herceptin, a first-line treatment for Her2-positive breast cancer.¹⁰ Efforts to better understand c-Src in the context of oncogenic growth, metastasis, and/or drug resistance have been complicated by a lack of selective c-Src inhibitors.^{11,12}

Our strategy involves modifying a promiscuous kinase inhibitor scaffold with an electrophile that targets a non-conserved cysteine of c-Src. This strategy was applied to two distinct promiscuously binding scaffolds. Our inhibitors represent the first irreversible inhibitors of wild-type c-Src,¹³ and these inhibitors show improved potency and selectivity relative to that of their reversible counterparts. We also demonstrate that irreversible inhibitors are able to overcome resistance mutations to the parent reversible scaffold. Finally, we demonstrate that irreversible inhibitors can be used to study protein conformation. Using an irreversible inhibitor, we study

the conformation of an important feature in inhibitor binding and selectivity, the phosphate-binding loop.

RESULTS AND DISCUSSION

Irreversible c-Src Inhibitor Design and Evaluation.

Protein kinases do not utilize active site cysteine residues in their catalytic cycle, and thus, irreversible kinase inhibitors must rely on noncatalytic cysteine residues in or adjacent to the ATP-pocket. c-Src has a nonconserved cysteine within its P-loop (phosphate-binding loop, or glycine-rich loop). This cysteine (Cys277 in c-Src, chicken numbering) is found in only nine (SRC, FGR, FGFR-1,2,3,4, LIMK1, TNK1, and YES) of the 518 human protein kinases, representing only 1.4% of all kinases (sequence alignment for kinases can be found in Supporting Information Figure S1).⁴ We reasoned that Cys277 of c-Src could be utilized to develop irreversible inhibitors of c-Src with improved potency and selectivity relative to their reversible analogues.

Our irreversible inhibitor design began with a previously reported, highly promiscuous kinase inhibitor based on an aminopyrazole scaffold.¹⁴ In the crystal structure (PDB: 3F6X),¹⁴ Cys277 is situated 10.6 Å away from the aminopyrazole (Figure 1). We synthesized an analogue of this promiscuous kinase inhibitor (compound 1). Profiling of compound 1 demonstrates promiscuous and potent binding to most kinases (see Supporting Information Figure S2 for

Received: July 7, 2012

Accepted: August 28, 2012

Published: August 28, 2012

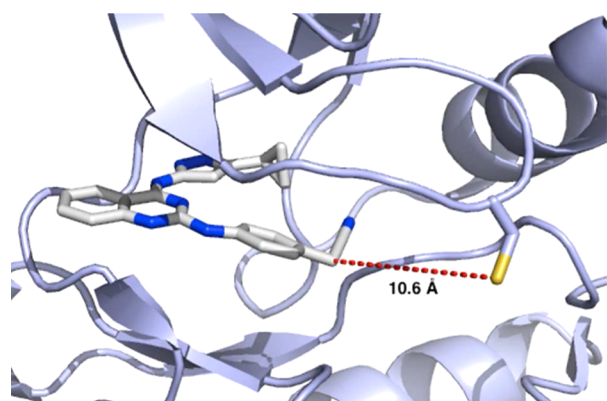


Figure 1. Crystal structure of c-Src bound to aminopyrazole inhibitor (PDB code: 3F6X). The sulfur in Cys277 is shown to be 10.6 Å from the inhibitor scaffold.

KINOMEScan profiling data). We reasoned that starting with a promiscuous inhibitor would be a particularly stringent test for improving selectivity through irreversible inhibition. Using compound **1** as the scaffold, we synthesized a series of analogues (compounds **2–7**) that contain a pendant electrophile with a linker of varied length. The linkers (glycine and β -alanine) and electrophiles (vinyl amide, α -chloro ketone, and vinyl sulfonamide) were used to produce a library of putative irreversible c-Src inhibitors with differing length and reactivity, respectively.

As an initial measure of potency, IC_{50} measurements were obtained at 0 and 120 min for the six putative irreversible inhibitors (Table 1). Compounds **2–7** each displayed time-dependent inhibition, while compound **1** showed identical inhibition at both 0 and 120 min using a previously reported continuous, fluorimetric activity assay.³⁵ Compounds **6** and **7** displayed the most significant c-Src inhibition at 120 min and were therefore selected for further study.

Evaluating Reversibility. To determine whether inhibitors **6** and **7** covalently interact with the P-loop Cys, further studies were performed. Time-dependent inhibition displayed by both compounds **6** and **7** is one trait of irreversible inhibitors.⁶ In addition, mutating Cys277 to Ser in c-Src leads to a significant loss of potency ($>6\times$) for both compounds **6** and **7**, while compound **1** has nearly identical potency for both WT c-Src and C277S c-Src (Table 2). This result indicates that potent inhibition requires Cys277. We then treated c-Src with compound **1**, **6**, or **7** and purified each complex by gel filtration. Kinase activity was regained with compound **1**; however, no kinase activity was observed for c-Src treated with **6** or **7** (see Supporting Information Figure S3). As a control, identical experiments performed with C277S c-Src and compound **7** demonstrated kinase activity was regained with inhibitor **7**. These results are consistent with **6** and **7** binding irreversibly and compound **1** binding reversibly.

Finally, the protein-inhibitor complexes for both compounds **6** and **7** with c-Src were analyzed by mass spectrometry, and after gel filtration, a single covalent adduct was found in both cases (see Supporting Information Figure S4). In contrast, no covalent adduct was observed when C277S c-Src was treated with compound **7**. Of note, the kinase domain of c-Src contains a total of six cysteine residues, and our data show covalent adduct formation only with Cys277. Together, these results clearly demonstrate that covalent binding of inhibitors **6** and **7** depends solely on the presence of Cys277.

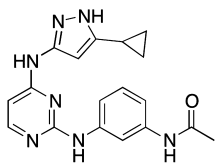
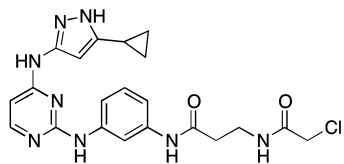
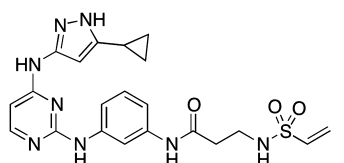
Table 1. IC_{50} Values for Compounds **1–7** against Wild-Type c-Src

Compound	R =	IC_{50} c-Src (nM)	
		0 min	120 min
1		667	720
2		4,376	352
3		3,240	341
4		1,694	569
5		3,229	611
6		1,219	91
7		760	93

Improved Selectivity with Irreversible Inhibition. Our compound design involves a promiscuous scaffold that reversibly binds to many off-targets; however, selectivity is expected to increase by improving binding for c-Src relative to the off-target kinases. We determined the selectivity of compounds **1**, **6**, and **7** using three homologous kinases (c-Src, c-Abl, and Hck) using a previously reported continuous, fluorimetric activity assay.³⁵ Obtaining selectivity between these three kinases has proven difficult in previous studies.¹¹ For example, a recent report using the KINOMEScan technology to profile 72 clinical and preclinical kinase inhibitors against a panel of 442 kinases indicated that no inhibitor in their panel has $>20\times$ selectivity for c-Src over both c-Abl and Hck.¹¹ Reversible aminopyrazole **1** is only *ca.* $3\times$ selective for c-Src over c-Abl and Hck. With irreversible inhibitors **6** and **7**, a significant increase in selectivity is observed (Table 2). Inhibitors **6** and **7** are both $>80\times$ selective for c-Src over c-Abl and $>65\times$ selective for c-Src over Hck. These results clearly demonstrate the ability of irreversible inhibition to markedly increase compound selectivity over off-target kinases lacking a P-loop Cys.

Selectivity between the nine kinases with this P-loop Cys is determined on the basis of the reversible scaffold employed. For example, irreversible inhibitors of FGFR were recently reported that rely on a P-loop Cys in the same position as Cys277 in c-Src; however, the FGFR inhibitors do not inhibit c-Src because the scaffold used does not inhibit c-Src.¹⁵ In our strategy, we utilize a highly promiscuous scaffold: kinome profiling indicates that compound **1** binds to all nine P-loop Cys containing kinases with measurable efficacy. Thus, we

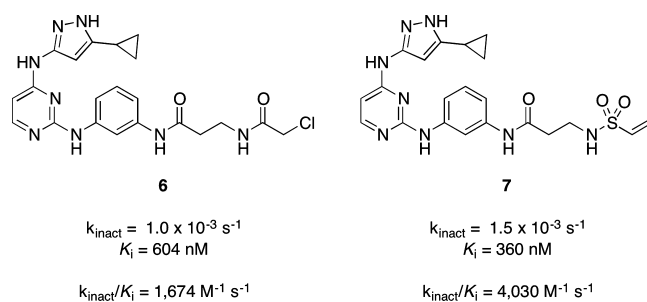
Table 2. IC₅₀ Values for Compounds 1, 6, and 7 against c-Src, c-Src C277S, c-Abl, c-Abl Q252C, and Hck at 120 min

Compound	IC ₅₀ c-Src	IC ₅₀ c-Src C277S	IC ₅₀ c-Abl	IC ₅₀ c-Abl Q252C	IC ₅₀ Hck
 1	720 nM	807 nM	2,108 nM	7,644 nM	2,753 nM
 6	91 nM	532 nM	9,090 nM	<100 nM	6,236 nM
 7	93 nM	1,237 nM	7,649 nM	145 nM	7,995 nM

anticipate that compounds 6 and 7 will inhibit each of the nine protein kinases with a P-loop Cys. To demonstrate this, we evaluated compound 7 with c-Yes and obtained an IC₅₀ of 46 nM (120 min), indicating that compound 7 is able to potently inhibit c-Yes. Modification of the reversible scaffold can provide irreversible inhibitors that can distinguish between kinases with a P-loop Cys.

Chemical Genetics To Target Kinases without a P-loop Cys. Our irreversible inhibitors were designed to covalently bind wild-type c-Src. However, we reasoned that mutagenesis of kinases without a P-loop cysteine (Xaa→Cys) would lead to irreversible inhibition with inhibitors 2–7. Because our design uses a highly promiscuous kinase inhibitor scaffold, this methodology can be directly applied to any of the kinases inhibited by aminopyrazole 1. To demonstrate the feasibility of this approach, we selected c-Abl. We produced c-Abl Q252C with a Cys in the analogous position to Cys277 in c-Src. While compounds 6 and 7 display modest, reversible inhibition for wild-type c-Abl, both 6 and 7 potently inhibit c-Abl Q252C (Table 2). Both compounds bind the Q252C mutant >55× better than wild-type c-Abl. Because the enzymatic activity is not altered by mutation within the P-loop,^{16,17} this strategy should be directly applicable to chemical genetic approaches for most kinases.

Determining k_{inact}/K_i . While irreversible inhibitors are often characterized using IC₅₀ values, these measurements are time-dependent and thus do not always report on true binding affinities.¹⁸ We determined both K_i and k_{inact} values for both irreversible inhibitors 6 and 7 to evaluate their affinity (K_i) and their rate of covalent bond formation with Cys277 (k_{inact}) (Figure 2).¹⁸ Briefly, we determined IC₅₀ values at RT with varied enzyme preincubation times, and k_{inact} and K_i values were then obtained directly from nonlinear regression of time-dependent IC₅₀ values as previously reported.¹⁸ We found that compound 7 has both better affinity ($K_i = 360$ nM) and faster rate constant for covalent bond formation ($k_{\text{inact}} = 1.5 \times 10^{-3}$ s⁻¹) compared to that of compound 6. IC₅₀ values were unable to discriminate between compounds 6 and 7; however, determination of k_{inact}/K_i demonstrates that compound 7 is

Figure 2. K_i and k_{inact} values for compounds 6 and 7.

the superior irreversible inhibitor. On the basis of these results, compound 7 was selected for further studies.

Evaluating Cellular Efficacy. In a cellular context, nucleophiles such as glutathione are present in high concentration and can potentially react with irreversible inhibitors to reduce covalent bonding to the target protein.⁶ To determine the effect of high concentrations of glutathione, we evaluated compound 7 in the presence of 1 mM reduced glutathione and found no change in biochemical IC₅₀ (see Supporting Information Figure S5). Similar results were obtained with adding a high concentration of DTT (1 mM). Thus, we observed that our irreversible inhibitor 7 is not reactive to exogenous nucleophiles. These results are consistent with studies that indicate that vinyl sulfonamides are kinetically slow substrates in intermolecular Michael reactions.¹⁹

To be useful as a biological probe, compound 7 must be able to inhibit Src activity *in cellulo*. We found that compound 7 is cell-permeable and able to inhibit cellular Src phosphorylation (see Supporting Information Figure S6). In addition, compound 7 was compared to reversible inhibitor 1 in a Src-dependent proliferation assay in 3D culture.²⁰ Reversible inhibitor 1 has a GI₅₀ of 14.3 μM, while irreversible inhibitor 7 has a GI₅₀ of 4.4 μM (see Supporting Information section XII). Thus, greater efficacy is observed for the irreversible inhibitor relative to its reversible counterpart. This increased efficacy parallels our biochemical studies that indicate irreversible inhibitors display greater potency for c-Src.

Application to Dasatinib Scaffold. Given the modular design of our irreversible inhibitor series, we reasoned that we could apply this strategy to other kinase inhibitor scaffolds that bind c-Src. Dasatinib is the only FDA-approved drug that potently inhibits c-Src and is generally considered a promiscuous kinase inhibitor (dasatinib binds to 52 kinases with $K_d < 100$ nM).¹¹ On the basis of our studies with the aminopyrazole scaffold, an irreversible dasatinib analogue should provide improved potency and selectivity for c-Src.

Analogues of dasatinib were synthesized with identical linker and electrophiles employed with irreversible inhibitors **6** and **7**, providing compounds **8** and **9**, respectively. Because dasatinib is such a tight binding inhibitor of c-Src (reported $K_i = 16$ pM),²¹ we were unable to fully characterize our irreversible inhibitors against wild-type c-Src due to enzyme requirements of our activity assay (dasatinib, **8**, and **9** have $IC_{50} < 5$ nM for WT c-Src at 0 min). c-Src with a gatekeeper mutation (T338M) is resistant to dasatinib binding ($IC_{50} = 14.3$ μ M, 120 min) and provides a means to evaluate our irreversible dasatinib analogues.²² We also prepared compound **10**, a reversible variant of compounds **8** and **9**, and found compound **10** was also a weak inhibitor of c-Src T338M. Unlike reversible inhibitors dasatinib and compound **10**, compounds **8** and **9** are both highly potent inhibitors of T338M c-Src (compound **8**: $IC_{50} = 5.5$ nM, 120 min; compound **9**: $IC_{50} = 44$ nM, 120 min, Figure 3). These results are significant because irreversible kinase inhibitors reported for wild-type FGFR1 were unable to efficiently inhibit FGFR1 with a gatekeeper Met (V561M).¹⁵

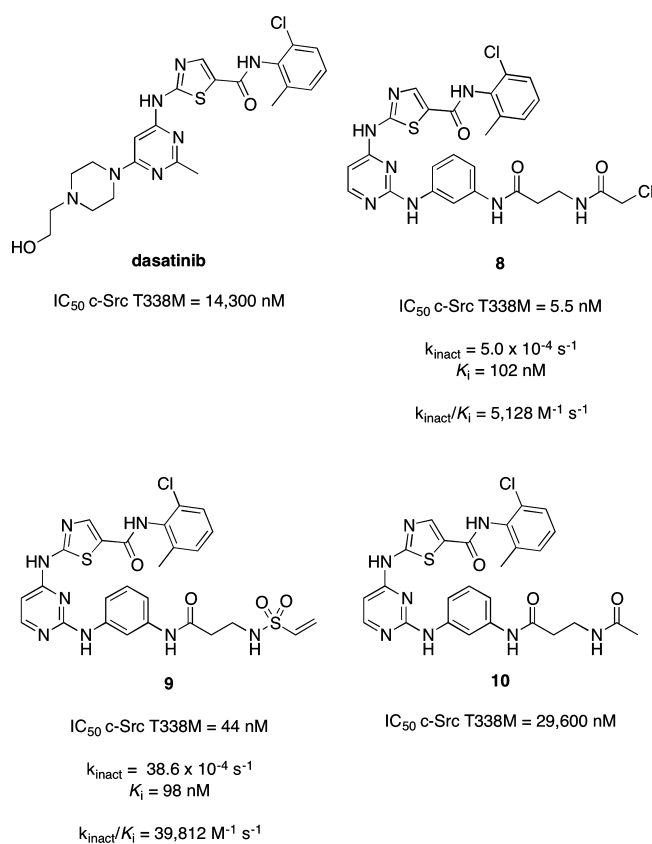


Figure 3. IC_{50} value for dasatinib and compounds **8**–**10** with c-Src T338M at 120 min and K_i and k_{inact} values for compounds **8** and **9** with c-Src T338M.

Here, we obtain highly potent irreversible inhibition for both wild-type and gatekeeper mutant c-Src.

Determining k_{inact} and K_i values for both compounds **8** and **9** demonstrated that **9** is a superior inhibitor with a k_{inact}/K_i value *ca.* 7 \times higher. Compounds **8** and **9** have similar K_i values. However, compound **9** covalently modifies (k_{inact}) T338M c-Src *ca.* 7 \times faster than does compound **8**. These results parallel the aminopyrazole scaffold in which the vinylsulfonamide-containing inhibitor covalently bound wild-type c-Src with greater inactivation rate constant (higher k_{inact}) compared to that of the α -chloro ketone. These results are also in agreement with predicted electrophilicity of vinyl sulfonamides and α -chloro ketones.²³ Compounds **8** and **9** are the most potent inhibitors of T338M c-Src reported to date and demonstrate the ability of irreversible kinase inhibitors to effectively inhibit mutant kinases with resistance to their reversible counterparts.

Selectivity of Compound 9. Kinome profiling has shown dasatinib to be a promiscuous inhibitor of tyrosine kinases.¹¹ We hypothesized that our irreversible dasatinib analogue (compound **9**) would display increased selectivity. Profiling of 131 kinases was performed at 15 nM ($5\times IC_{50}$ in this assay) dasatinib or compound **9** using a 2 h incubation (Lucoome Biotechnologies).^{24,25} Selectivity differences between compounds can be compared by their S -score.²⁶ S -score represents the fraction of kinases inhibited to a particular level (S_{35} is the number of kinases with <35% of control activity divided by the total number of nonmutant kinases in the panel, here 124). In this panel, dasatinib has $S_{35} = 0.12$ and $S_{15} = 0.08$ at 15 nM (Table 3). Compound **9** has $S_{35} = 0.07$ and $S_{15} = 0.03$ at 15 nM.

Table 3. Selectivity Scores for Dasatinib and Compound **9** against a Panel of 131 Diverse Kinases

compound	S_{15}	S_{35}
dasatinib	0.08	0.12
9	0.03	0.07

These data indicate that, as predicted, compound **9** has significantly improved selectivity compared to that of dasatinib (lower S -score indicates higher selectivity). Full kinome profiling data can be found in the Supporting Information Section XV.

We were interested in whether compound **9** would display binding to kinases with a P-loop Cys (see Supporting Information Figure S1 for sequence alignment of kinases with P-loop Cys). Five of the nine kinases with this P-loop Cys are present in the Lucoome panel (SRC, YES, FGFR1, FGFR2, and LIMK1). Both c-Src and c-Yes are very potently inhibited by dasatinib; however, dasatinib does not display binding to FGFR1, FGFR2, or LIMK1.¹¹ Compound **9** only weakly binds FGFR2 (78.7% of control (POC)), and no binding of compound **9** was observed to either FGFR1 or LIMK1. These data indicate that the reversible scaffold selectivity largely determines which of the kinases containing a P-loop Cys will be inhibited. Thus, with appropriate selection of the scaffold, it is possible to obtain selectivity between the nine kinases with a P-loop Cys.

In our panels, TEC and TXK kinases display increased binding with compound **9** compared to that of dasatinib. Notably, both TEC and TXK contain a Cys residue in their sugar-binding pockets.⁴ While both TEC and TXK were only modestly inhibited by compound **9** (TEC = 48.6 POC, TXK = 54.1 POC), these data indicate that it is possible to irreversibly

inhibit off-target kinases with Cys located elsewhere in the kinase domain. Furthermore, with modification of the core scaffold (dasatinib is a weak binder of both TEC and TXK) and modification of the linker length, it should be possible to develop highly potent irreversible inhibitors for each of these kinases using our strategy.

Cellular Efficacy of Compound 9. Compound 9 efficiently reduced the proliferation of HT-29 colon cancer cells growing *in vitro* ($GI_{50} = 224$ nM). This GI_{50} is comparable to reported values for growth inhibition of HT-29 cells by dasatinib.²⁷ We next examined the efficacy of compound 9 against a breast cancer cell line known to be growth-dependent upon c-Src (SKBR3).^{12,28} In SKBR3 cells, compound 9 was an efficacious inhibitor ($GI_{50} = 91$ nM), while dasatinib was less potent ($GI_{50} = 1.6$ μ M). As demonstrated with compound 7, irreversible inhibitors of c-Src can perform with greater cellular efficacy than their reversible counterpart, which is an important criterion for their use as biological probes. We also measured the toxicity of dasatinib and compound 9 to noncancer cells using primary human mammary cells (HMEC) and found the off-target cellular toxicity to be similar (2.3 and 1.0 μ M, respectively, see Supporting Information section XII).

Insight into P-Loop Conformation Using Irreversible Inhibitors. The P-loop of kinases is a highly flexible and dynamic structure.^{29,30} P-loop conformation has been proposed to be responsible for drug selectivity and resistance in kinases.^{17,29} Because irreversible inhibitors can report on the rate of inactivation (k_{inact}),¹⁸ we reasoned that the time scale of these rate constants should provide us with a simplified model to study the conformation of the P-loop. Importantly, k_{inact} values are independent of binding affinity (K_i),¹⁸ enabling their use in deciphering protein conformation. Thus, k_{inact} values can report on the distance from inhibitor electrophile to Cys nucleophile.⁶

Crystal structures of enzyme-dasatinib complexes indicate that c-Src has an extended P-loop conformation while c-Abl's P-loop is kinked (Figure 4).³⁰ We determined k_{inact} values for inactivation by compound 7 of both c-Src and c-Abl Q252C. Consistent with the crystal structure conformation, we

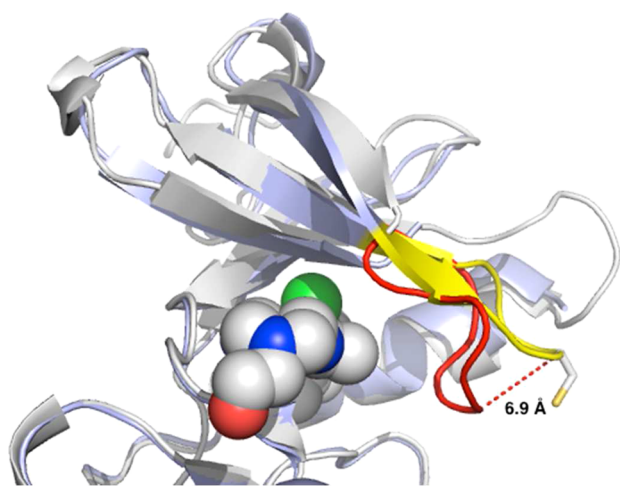


Figure 4. Alignment of structures with dasatinib bound to c-Src (PDB code: 3QLG) and c-Abl (2GQG). c-Src is colored light blue with the P-loop of c-Src highlighted in yellow. c-Abl is colored light gray with the P-loop of c-Abl highlighted in red. Dasatinib is shown as a space fill model.

observed that the k_{inact} for c-Abl Q252C was *ca.* 2 \times larger than the inactivation rate constant for c-Src (Figure 5). This

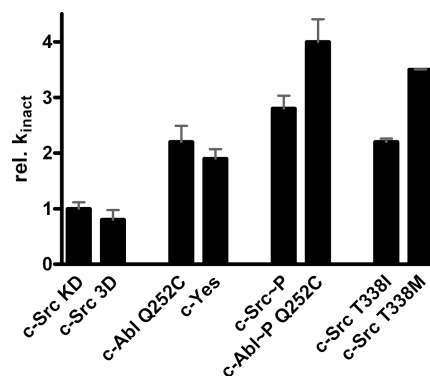


Figure 5. Relative k_{inact} values for compound 7. Statistical analysis was performed in GraphPad Prism 4.0 using a two-tailed *t* test (c-Src KD vs c-Abl Q252C, $p < 0.05$; c-Src KD vs c-Yes, $p < 0.05$; c-Src KD vs c-Src~P, $p < 0.01$; c-Abl Q252C vs c-Abl~P Q252C, $p < 0.01$; c-Src KD vs c-Src T338I, $p < 0.01$; c-Src KD vs c-Src T338M, $p < 0.005$).

statistically significant ($p < 0.05$) difference likely results from the kinked conformation of c-Abl's P-loop, which positions Cys252 closer to the vinyl sulfonamide of compound 7 (with dasatinib bound, c-Abl's P-loop is 6.9 Å closer to the aminopyrazole core than the P-loop of dasatinib-bound c-Src, Figure 4).

We recently reported a series of reversible c-Src inhibitors that were designed to interact with the "P-loop pocket" of c-Src.¹² We obtained highly specific inhibitors for c-Src that were unable to bind tightly to both c-Abl and c-Yes.¹² Our hypothesis, consistent with crystal structures for c-Src and c-Abl, is that the P-loop conformation controls selectivity for this class of inhibitors.²⁹ Because neither a crystal structure of c-Yes nor computational prediction of the P-loop of c-Yes has been reported, we employed our method to study the c-Yes P-loop conformation. We found that compound 7 inactivated c-Yes with a rate constant (k_{inact}) nearly identical to the inactivation rate constant for c-Abl. Consistent with our previously reported work,¹² these data indicate that c-Yes likely has a kinked P-loop conformation. This hypothesis is intriguing given the high sequence similarity between c-Src and c-Yes (95% similarity, 90% identity).

In protein kinases, stabilization of the active kinase conformation has been reported to cause movement of the kinase P-loop.^{31,32} We hypothesized that phosphorylation of the activation loop, which stabilizes the active conformation, would lead to divergent rates of covalent modification of the P-loop Cys. We determined k_{inact} values for c-Src~pTyr416 (c-Src~P) and found the inactivation rate constant was *ca.* 2 \times larger in c-Src~P relative to that of wild-type c-Src (Figure 5). This trend was also observed in c-Abl Q252C, where the inactivation rate was *ca.* 2 \times higher for the phosphorylated protein. These data suggest that the P-loop conformation of both c-Src and c-Abl Q252C is more closed on stabilization of the active kinase conformation (a larger rate constant implies closer distance between electrophile and nucleophile).

We next wanted to explore the role of gatekeeper mutation on P-loop conformation. Gatekeeper mutations in a kinase generally increase the affinity for ATP relative to wild-type kinase.¹⁷ We hypothesized that this increase in affinity for ATP might result from movement of the P-loop. Thus, we

determined inactivation rate constants (k_{inact}) for T338I and T338M c-Src (Figure 5). In both cases, we found that mutation of the gatekeeper residue of c-Src (to either Ile or Met) caused a $>2\times$ increase in k_{inact} ($p < 0.01$). On the basis of these results, we propose that the gatekeeper mutation leads to closure of the P-loop. The mechanism by which the gatekeeper residue can alter the P-loop conformation is unknown; however, molecular dynamics simulations with c-Abl and EGFR have reported that the gatekeeper mutation causes movement of both the α C-helix and the P-loop.^{33,34} This model is consistent with our data and supports our hypothesis that gatekeeper mutation leads to a more closed P-loop conformation in c-Src.

Herein, we have demonstrated that inactivation rate constants (k_{inact}) for irreversible inhibitors may be utilized to study the conformation of the kinase P-loop. While changes in k_{inact} could be due to a number of factors, we believe the major contributor to k_{inact} differences is P-loop conformation. Our approach is consistent with crystal structures of c-Src and c-Abl with regard to the P-loop conformation. We applied this method to study the conformation of the c-Yes P-loop, and consistent with previously reported results from our laboratory,¹² we believe that c-Yes has a closed P-loop conformation. Using k_{inact} data, we further hypothesize that both phosphorylation of the activation loop and gatekeeper mutation leads to increased kinking of the P-loop. To our knowledge, this represents the first use of irreversible inhibitors in this context, and we believe this technique should be valuable for the further study of protein kinase conformation.

Conclusion. We have reported the development and characterization of the first irreversible inhibitors of wild-type c-Src. Our method to generate irreversible inhibitors of c-Src involves modification of a known (and promiscuous) scaffold by appending an electrophile positioned to covalently modify a nonconserved cysteine in the P-loop of c-Src. We applied this method to two distinct scaffolds and identified irreversible inhibitors for each scaffold. When compared to their reversible counterparts, our irreversible inhibitors were found to be significantly more potent and selective in biochemical assays. Cellular assays demonstrate that our irreversible inhibitors are more efficacious than reversible inhibitors in inhibiting c-Src *in cellulo*. We also demonstrated the applicability of our method to kinases without a natural cysteine residue in their P-loop using chemical genetic techniques. Finally, we established the utility of irreversible inhibitors in studying kinase P-loop conformation using rates of irreversible inactivation (k_{inact}). Application to three kinases and three c-Src constructs provides insight into the how the P-loop conformation is altered by mutagenesis or between kinases. These results can aid in understanding why P-loop conformation affects inhibitor selectivity and drug resistance.^{12,29} Together, our results demonstrate straightforward and general methodology for developing irreversible kinase inhibitors.

METHODS

Synthesis of Compounds 1–10. Synthetic schemes, detailed procedures, and characterization of compounds 1–10 can be found in the Supporting Information.

Biochemical Inhibition Assays. To determine inhibitor efficacy, we utilized a previously reported continuous, fluorimetric assay.³⁵ Briefly, phosphorylation of a self-reporting peptide substrate causes a fluorescence emission increase at 405 nm (ex. 340 nm). Final assay concentrations were as follows: ATP = 100 μ M, substrate peptide = 45 μ M. For more information and dose–response curves for each compound, see Supporting Information section VI.

Determination of k_{inact}/K_i . We determined IC₅₀ values at RT with varied enzyme preincubation times (2, 10, 20, 30, 45, 60, 75, 90, 105, 120 min). For k_{inact} and K_i determination, the values were obtained directly from nonlinear regression of time-dependent IC₅₀ values as previously reported.¹⁸ See Supporting Information section VIII for additional information.

Production of c-Src T338M, T338I. Chicken c-Src kinase domain in pET28a, modified with a TEV protease cleavable N-terminal 6x-His tag was prepared as previously reported.³⁶ The desired mutation (either T338M or T338I) was added to this plasmid using the Agilent QuikChange II kit. The plasmid was transformed by electroporation into BL21DE3 electrocompetent cells containing YopH expression vector in pCDFDuet-1. Cell growth and expression and protein purification were performed using modified literature protocols for expression of wild-type c-Src kinase domain.³⁶

Production of c-Abl Q252C. c-Abl kinase domain in pET28a, modified with a TEV protease cleavable N-terminal 6x-His tag was prepared as previously reported.³⁶ The Q252C mutation was added to this plasmid using the Agilent QuikChange II kit. The plasmid was transformed by electroporation into BL21DE3 electrocompetent cells containing YopH expression vector in pCDFDuet-1. Cell growth, expression, and protein purification were performed using modified literature protocols for expression of wild-type c-Abl kinase domain.³⁶

v-Src/3T3 Cell Growth Assays in 3D Culture. Prior to plating cells, 50 μ L Cultrex basement membrane extract (BME, Trevigen) was added to each well of a 96-well plate incubated on ice and then allowed to gel (cushion formation) over a 30 min time period in a 37 °C incubator. v-Src 3T3 cells were then dispersed from flasks and collected by centrifugation (200 \times g for 5 min at RT). An aliquot of the resuspended cells was mixed with trypan blue solution, and the cell number was quantified using a hemacytometer. Next 100% DMSO compound stocks were prepared to 100 \times the final concentration that is desired in the assay. Three microliters of the DMSO stock solution was then added to 297 μ L of the cell suspension supplemented with 5% BME to give a DMSO concentration of 1%. The cells were plated at about 1.0×10^4 cells per well (100 μ L/well) in triplicate for each compound concentration. The plate was then placed within the IncuCyte imager in the 37 °C, 5% CO₂ humidified incubator, and camera images were taken every 2 h to measure confluency percentages over time. The data was plotted as a percentage of the vehicle (1% DMSO alone), and analysis and curve fitting was performed using GraphPad Prism. Kinetic growth curves were based off of the first 24 h of cell growth inhibition and used to construct GI₅₀ curves.

Cell Growth Inhibition Assays. Cancer cell lines (obtained from ATCC) were dispersed from 70–80% confluent monolayer cultures using 0.25% trypsin-EDTA and plated in 96-well microtiter plates at $5.0\text{--}7.0 \times 10^3$ cells per well. The cells were allowed to attach for 24 h in medium (DMEM, 10% FBS, 1X pen/strep) at 37 °C in a humidified incubator with 5% CO₂. After 24 h, the growth medium was replaced with medium (DMEM, 10% FBS, no antibiotic) containing compound to be tested at 1% DMSO final concentration. Medium and compound were replaced every 24 h. After 72 h, WST-1 (Roche Applied Science) was added according to the manufacturer's procedure and incubated for 60 min. After incubation, absorbance readings at 450 and 630 nm were taken. Data analysis and curve fitting was performed using Graphpad Prism software. See Supporting Information section XII for dose–response curves.

Kinome Profiling of Compound 9. Kinome profiling of dasatinib and compound 9 was performed by Luceome Biotechnologies (Tucson, AZ).^{24,25} To select an appropriate concentration, IC₅₀ values for dasatinib and compound 9 were obtained using the Luceome technology. Nearly identical IC₅₀ values were obtained (3.1 nM for dasatinib, 3.7 nM for compound 9). Both dasatinib and compound 9 were profiled at a concentration of 15 nM. Full profiling results are available in the Supporting Information section XV.

■ ASSOCIATED CONTENT

■ Supporting Information

Supplementary figures, experimental methods, and characterization of compounds 1–10. This material is available free of charge via the Internet at <http://pubs.acs.org>.

■ AUTHOR INFORMATION

Corresponding Author

*E-mail: soellner@umich.edu.

Notes

The authors declare no competing financial interest.

■ ACKNOWLEDGMENTS

We thank M. Seeliger (SUNY, Stony Brook) and J. Kuriyan (UC Berkeley) for providing expression plasmids for ABL, HCK, and SRC. We thank K. Shokat (UCSF) for providing v-Src/3T3 stably transfected cell line. We thank A. Mapp (U. Michigan) for helpful discussions. F.E.K. was supported by a National Institutes of Health Chemistry-Biology Interface Training Grant (T32GM008597). We thank the National Institutes of Health (R01GM088546 to M.B.S.) and the University of Michigan College of Pharmacy for support of this work.

■ REFERENCES

- (1) Levitzki, A., and Gazit, A. (1995) Tyrosine kinase inhibition—an approach to drug development. *Science* 267, 1782–1788.
- (2) Manning, G., Whyte, D. B., Martinez, R., Hunter, T., and Sudarsanam, S. (2002) The protein kinase complement of the human genome. *Science* 298, 1912–1934.
- (3) Knight, Z. A., and Shokat, K. M. (2005) Features of selective kinase inhibitors. *Chem. Biol.* 12, 621–637.
- (4) Zhang, J. M., Yang, P. L., and Gray, N. S. (2009) Targeting cancer with small molecule kinase inhibitors. *Nat. Rev. Cancer* 9, 28–39.
- (5) Leproult, E., Barluenga, S., Moras, D., Wurtz, J.-M., and Winssinger, N. (2011) Cysteine mapping in conformationally distinct kinase nucleotide binding sites: application to the design of selective covalent inhibitors. *J. Med. Chem.* 54, 1347–1355.
- (6) Barf, T., and Kaptein, A. (2012) Irreversible protein kinase inhibitors: balancing the benefits and risks. *J. Med. Chem.* 55, 6243–6262.
- (7) Singh, J., Petter, R. D., and Kluge, A. F. (2010) Targeted covalent drugs of the kinase family. *Curr. Opin. Chem. Biol.* 14, 475–480.
- (8) Thomas, S. M., and Brugge, J. S. (1997) Cellular functions regulated by Src family kinases. *Ann. Rev. Cell. Dev. Biol.* 13, 513–609.
- (9) Martin, G. S. (2001) The hunting of the Src. *Nat. Rev. Mol. Cell. Biol.* 2, 467–475.
- (10) Zhang, S., Huang, W.-C., Li, P., Guo, H., Poh, S.-B., Brady, S. W., Xiong, Y., Tseng, L.-M., Li, S.-H., Ding, Z., Sahin, A. A., Estevam, F. J., Hortobagyi, G. N., and Yu, D. (2011) Combating trastuzumab resistance by targeting SRC, a common node downstream of multiple resistance pathways. *Nat. Med.* 17, 461–469.
- (11) For a recent survey of kinase inhibitor selectivity, see: Davis, M. I., Hunt, J. P., Herrgard, S., Ciceri, P., Wodicka, L. M., Pallares, G., Hocker, M., Treiber, D. K., and Zarrinkar, P. P. (2011) Comprehensive analysis of kinase inhibitor selectivity. *Nat. Biotechnol.* 29, 1046–1051.
- (12) Brandvold, K. B., Steffey, M. E., Fox, C. C., and Soellner, M. B. (2012) Development of a highly selective c-Src kinase inhibitor. *ACS Chem. Biol.* 7, 1393–1398.
- (13) For an irreversible inhibitor against non-native c-Src, see: (a) Blair, J. A., Rauh, D., Kung, C., Yun, C.-H., Fan, Q.-W., Rode, H., Zhang, C., Eck, M. J., Weiss, W. A., and Shokat, K. M. (2007) Structure-guided probes for tyrosine kinases using chemical genetics. *Nat. Chem. Biol.* 3, 229–238. (b) Garske, A. L., Peters, U., Cortesi, A. T., Perez, J. L., and Shokat, K. M. (2011) Chemical genetic strategy for targeting protein kinases based on covalent complementary. *Proc. Natl. Acad. Sci. U.S.A.* 108, 15046–15052.
- (14) Statsuk, A. V., Maly, D. J., Seeliger, M. A., Fabian, M. A., Biggs, W. H., III, Lockhart, D. J., Zarrinkar, P. P., Kuryan, J., and Shokat, K. M. (2008) Tuning a three-component reaction for trapping kinase substrate complexes. *J. Am. Chem. Soc.* 130, 17568–17574.
- (15) Zhou, W., Hur, W., McDermott, L., Dutt, A., Xian, W., Ficarro, S. B., Zhang, J., Sharma, S. V., Brugge, J., Meyerson, M., Settleman, J., and Gray, N. S. (2010) A structure-guided approach to creating covalent FGFR inhibitors. *Chem. Biol.* 17, 285–295.
- (16) Seeliger, M. A., Ranjitkar, P., Kasap, C., Shan, Y., Shaw, D. E., Shah, N. P., Kuriyan, J., and Maly, D. J. (2009) Equally potent inhibition of c-Src and c-Abl by compounds that recognize inactive kinase conformations. *Cancer Res.* 69, 2384–2392.
- (17) Krishnamurthy, R., and Maly, D. J. (2010) Biochemical mechanisms of resistance to small-molecule protein kinase inhibitors. *ACS Chem. Biol.* 5, 121–138.
- (18) Krippendorff, B.-F., Neuhaus, R., Lienau, P., Reichel, A., and Huisinga, W. (2009) Mechanism-based inhibition: deriving K_i and k_{inact} directly from time-dependent IC_{50} values. *J. Biomol. Screening* 14, 913–923.
- (19) Reddick, J. J., Cheng, J., and Roush, W. R. (2003) Relative rates of Michael reactions of 2'-(phenyl)thiol with vinyl sulfones, vinyl sulfonate esters, and vinyl sulfonamides relevant to vinyl sulfone cysteine protease inhibitors. *Org. Lett.* 5, 1967–1970.
- (20) Hauck, C. R., Hsia, D. A., Puente, X. S., Cheres, D. A., and Schlaepfer, D. D. (2002) FRNK blocks v-Src-stimulated invasion and experimental metastases without effects on cell motility or growth. *EMBO J.* 21, 6289–6302.
- (21) Lombardo, L. J., Lee, F. Y., Chen, P., Norris, D., Barrish, J. C., Behnia, K., Castaneda, S., Cornelius, L. A., Das, J., Doweiko, A. M., Farichild, C., Hunt, J. T., Inigo, I., Johnston, K., Kamath, A., Kan, D., Klei, H., Marathe, P., Pang, S., Peterson, R., Pitt, S., Schieven, G. L., Schmidt, R. J., Tokarski, J., Wen, M. L., Wityak, J., and Borzilleri, R. M. (2004) Discovery of N-(2-chloro-6-methyl-phenyl)-2-(6-(4-(2-hydroxyethyl)-piperazin-1-yl)-2-methylpyrimidin-4-ylamino)thiazole-5-carboxamide (BMS-354825), a dual Src/Abl kinase inhibitor with potent antitumor activity in preclinical assays. *J. Med. Chem.* 47, 6658–6661.
- (22) Getlik, M., Grutter, C., Simard, J. R., Kluter, S., Rabiller, M., Rode, H. B., Robubi, A., and Rauh, D. (2009) Hybrid compound design to overcome the gatekeeper T338M mutation in cSrc. *J. Med. Chem.* 52, 3915–3926.
- (23) Kluter, S., Simard, J. R., Rode, H. B., Grutter, C., Pawar, V., Raaijmakers, H. C. A., Bard, T. A., Rabiller, M., van Otterlo, W. A. L., and Rauh, D. (2010) Characterization of irreversible kinase inhibitors by directly detecting covalent bond formation: a tool for dissecting kinase drug resistance. *ChemBioChem* 11, 2557–2566.
- (24) Jester, B. W., Cox, K. J., Gaj, A., Shomin, C. D., Porter, J. D., and Ghosh, I. (2010) A coiled-coil enabled split-luciferase three-hybrid system: applied toward profiling inhibitors of protein kinases. *J. Am. Chem. Soc.* 132, 11727–11735.
- (25) Jester, B. W., Gaj, A., Shomin, C. D., Cox, K. J., and Ghosh, I. (2012) Testing the promiscuity of commercial kinase inhibitors against the AGC kinase group using a split-luciferase screen. *J. Med. Chem.* 55, 1526–1537.
- (26) Karaman, M. W., Herrgard, S., Treiber, D. K., Gallant, P., Atteridge, C. E., Campbell, B. T., Chan, K. W., Ciceri, P., Davis, M. I., Edeen, M. I., Edeen, P. T., Faraoni, R., Floyd, M., Hunt, J. P., Lockhart, D. J., Milanov, Z. V., Morrison, M. J., Pallares, G., Patel, H. K., Pritchard, S., Woficka, L. M., and Zarrinkar, P. P. (2008) A quantitative analysis of kinase inhibitor selectivity. *Nat. Biotechnol.* 26, 127–132.
- (27) Holbeck, S. L., Collins, J. M., and Doroshow, J. H. (2010) Analysis of FDA-approved anti-cancer agents in the NCI60 panel of human tumor cell lines. *Mol. Cancer Ther.* 9, 1451–1460.
- (28) Zheng, X., Resnick, R. J., and Shalloway, D. (2008) Apoptosis of estrogen-receptor negative breast cancer and colon cancer cell lines by PTPa and Src RNAi. *Int. J. Cancer* 122, 1999–2007.

(29) For a recent review, see: Patel, R. Y., and Doerksen, R. J. (2010) Protein Kinase—inhibitor database: Structural variability of and inhibitor interactions with the protein kinase P-loop. *J. Proteome Res.* 9, 4433–4442.

(30) Guimaraes, C. R. W., Rai, B. K., Munchhof, M. J., Liu, S., Wang, J., Bhattacharya, S. K., and Buckbinder, L. (2011) Understanding the impact of P-loop conformation on kinase selectivity. *J. Chem. Inf. Model.* 51, 1199–1204.

(31) Hubbard, S. R. (1997) Crystal structure of the activated insulin receptor tyrosine kinase in complex with peptide substrate and ATP analog. *EMBO J.* 16, 5572–5581.

(32) Vajpai, N., Strauss, A., Fendrich, G., Cowan-Jacob, S. W., Manley, P. W., Grzesiek, S., and Jahnke, W. (2008) Solution conformations and dynamics of ABL kinase-inhibitor complexes determined by NMR substantiate the different binding modes of imatinib/nilotinib and dasatinib. *J. Biol. Chem.* 283, 18292–18302.

(33) Lee, T.-S., Potts, S. J., Kantarjian, H., Cortes, J., Giles, F., and Albitar, M. (2008) Molecular basis explanation for imatinib resistance of BCR-ABL due to T315I and P-loop mutations from molecular dynamics simulations. *Cancer* 112, 1744–1753.

(34) Dixit, A., and Verkhiver, G. M. (2009) Hierarchical modeling of activation mechanisms in the ABL and EGFR kinase domains: thermodynamic and mechanistic catalysts of kinase activation by cancer mutations. *PLoS Comp. Biol.* 5, 1–22.

(35) Wang, Q., Cahill, S. M., Blumenstein, M., and Lawrence, D. S. (2006) Self-reporting fluorescent substrates of protein tyrosine kinases. *J. Am. Chem. Soc.* 128, 1808–1809.

(36) Seeliger, M. A., Young, M., Henderson, M. N., Pellicena, P., King, D. S., Falick, A. M., and Kuriyan, J. (2005) High yield bacterial expression of active c-Abl and c-Src tyrosine kinases. *Protein Sci.* 14, 3135–3139.